



Published in final edited form as:

Conf Proc IEEE Eng Med Biol Soc. 2011 August ; 2011: 8444–8447. doi:10.1109/IEMBS.2011.6092083.

Instantaneous Assessment of Autonomic Cardiovascular Control during General Anesthesia

Zhe Chen[Senior Member, IEEE], **Luca Citi**[Member, IEEE], **Patrick L Purdon**[Member, IEEE], **Emery N Brown**[Fellow, IEEE], and **Riccardo Barbieri**^{*}[Senior Member, IEEE]

The authors are with the Neuroscience Statistics Research Laboratory, Massachusetts General Hospital, Harvard Medical School, Boston, MA 02114, USA. E. N. Brown is also with the Harvard-MIT Division of Health Science and Technology and the Department of Brain and Cognitive Sciences, Massachusetts Institute of Technology, Cambridge, MA 02139, USA

Abstract

We present a comprehensive probabilistic point process framework to estimate and monitor the instantaneous heartbeat dynamics as related to specific cardiovascular control mechanisms and hemodynamics. Assessment of the model's statistics is established through the Wiener-Volterra theory and a multivariate autoregressive (AR) structure. A variety of instantaneous cardiovascular metrics, such as heart rate (HR), heart rate variability (HRV), respiratory sinus arrhythmia (RSA), and baroreceptor-cardiac reflex (BRS), can be rigorously derived within a parametric framework and instantaneously updated with an adaptive algorithm. Instantaneous metrics of nonlinearity, such as the bispectrum of heartbeat intervals, can also be derived. We have applied the proposed point process framework to experimental recordings from healthy subjects in order to monitor cardiovascular regulation under propofol anesthesia. Results reveal interesting dynamic trends across different pharmacological interventions, confirming the ability of the algorithm to track important changes in cardiorespiratory elicited interactions, and pointing at our mathematical approach as a promising monitoring tool for an accurate, noninvasive assessment of general anesthesia.

I. INTRODUCTION

In recent years, advanced statistical models have been developed for evaluating the heartbeat dynamics [1–3]. Heartbeats, once detected from continuous electrocardiogram (ECG) signal, are treated as discrete events that can be modeled by a stochastic point process [2, 3].

Various probabilistic models (e.g., the inverse Gaussian, Gaussian, lognormal, or gamma distribution) can be used to model the heartbeat interval [4], whereas its mean is modulated by previous inter-beat intervals. Nonlinearity of the heartbeat dynamics, as well as the interactions between the heartbeat and other cardiovascular measures, have always been subject of important studies in the last decades. In light of the Wiener-Volterra theory, we present a comprehensive point process framework to include the interactions between the heartbeat intervals and other cardiovascular measures such as respiration and arterial blood pressure, as well as assessing nonlinear heartbeat dynamics.

^{*}R Barbieri is the corresponding author (Barbieri@neurostat.mit.edu).

II. METHODS

A. The Heartbeat Interval Point Process Model

Given a set of R-wave events $\{u_j\}_{j=1}^J$ detected from the electrocardiogram (ECG), let $RR_j = u_j - u_{j-1} > 0$ denote the j^{th} R-R interval. By treating the R-waves as discrete events, we develop a point process model for the heartbeat interval. Assuming history beat dependence, the waiting time $t - u_j$ ($t > u_j$) until the next R-wave event can be modeled by an inverse Gaussian model [2]:

$$p(t) = \left(\frac{\theta}{2\pi(t-u_i)^3} \right)^{\frac{1}{2}} \exp \left(-\frac{\theta(t-u_i - \mu_{RR}(t))^2}{2(t-u_i)\mu_{RR}^2(t)} \right) \quad (1)$$

where u_j denotes the previous R-wave event occurred before time t , $\theta > 0$ denotes the shape parameter, and $\mu_{RR}(t)$ denotes the instantaneous R-R mean. As HR is defined as the reciprocal of RR, by the *change-of-variables* formula, the mean and the standard deviation

of HR can be derived [2], as given by $\mu_{HR} = \tilde{\mu}^{-1} + \tilde{\theta}^{-1}$ and $\sigma_{HR} = \sqrt{(2\tilde{\mu} + \tilde{\theta})/\tilde{\mu}\tilde{\theta}^2}$ where $\tilde{\mu} = c^{-1} \mu_{RR}$, and $c = 60$ s/min.

B. Modeling the Instantaneous Mean Heartbeat Interval

In general, let us consider a causal, continuous-time nonlinear mapping F between an output variable $y(t)$ and two input variables $x(t)$ and $u(t)$. Expanding the Wiener-Volterra series of function F (up to the second order) with respect to inputs $x(t)$ and $u(t)$ yields to a sum of first and second order convolutions of the inputs with Volterra kernels of appropriate orders [7]. In our model, $y(t)$ will be replaced by $\mu_{RR}(t)$, $x(t)$ will be replaced by the previous R-R intervals, $u(t)$ will be replaced by either BP or RESP, or both, and the continuous-time integral will be approximated by a finite and discrete approximation. Our framework considers three important cases:

Case 1: Univariate Model. Dropping off the terms that involve all of covariate terms in the Volterra series expansion, we obtain a discrete-time system:

$$\mu_{RR}(t) = a_0(t) + \sum_{i=1}^p a_i(t) RR_{t-i} + \sum_{i=1}^r \sum_{j=1}^r h_{ij}(t) \overline{RR}_{t-i} \overline{RR}_{t-j} \quad (2)$$

where the first two terms represent a linear autoregressive (AR) model of the past R-R intervals, $a_0(t)$ compensates the nonzero mean effect of the R-R measurements, and

$$\overline{RR}_t = RR_t - 1/\ell \sum_{k=1}^{\ell} RR_{t-k} \quad (\ell = \max\{p, r\})$$

Case 2: Multivariate Model. Dropping off the last two quadratic terms in the Volterra series expansion, we obtain

$$\mu_{RR}(t) = \tilde{a}_0(t) + \sum_{i=1}^p \tilde{a}_i(t) RR_{t-i} + \sum_{j=1}^p \tilde{b}_j(t) COV_{t-j} + \sum_{i=1}^r \sum_{j=1}^r \tilde{h}_{ij}(t) \overline{RR}_{t-i} \overline{COV}_{t-j} \quad (3)$$

which yields a bivariate bilinear system. Here the covariate $COV = [BP \text{ RESP}]$ measurements are assumed to have the mean subtracted as for RR in (2) [16].

Case 3: ARIMA (ARX on the differences) Linear Multivariate Model. We define the “increment of the R-R series” $\{\delta RR_{t-i}\} \equiv \{RR_{t-i} - RR_{t-i-1}\}$ and the “increment of the covariate series” $\{\delta COV_{t-i}\} \equiv \{COV_{t-i} - COV_{t-i-1}\}$, and model the instantaneous heartbeat interval mean by

$$\mu_{RR}(t) = RR_{t-1} + \sum_{i=1}^p \hat{a}_i(t) \delta RR_{t-i} + \sum_{j=1}^p \hat{b}_j(t) \delta COV_{t-j} \quad (4)$$

where $\tilde{a}_0(t)$ in (3) has been replaced by RR_{t-1} in (4) [8].

C. Frequency Analysis

From Equation (2), the instantaneous R-R spectrum of the linear part is

$$\mathcal{D}_{RR}(f, t) = \frac{\sigma_{RR}^2(t)}{\left| 1 - \sum_{i=1}^p a_i(t) z^{-i} \right|_{z=e^{j2\pi f}}} \quad (5)$$

With the time-varying AR coefficients $\{a_i(t)\}$ estimated from the point-process filter, we may evaluate the *spectral power* of Eq. (5) at different ranges (LF, 0.04–0.15 Hz; HF, 0.15– $\min\{0.5, 0.5/RR\}$ Hz, where $0.5/RR$ denotes the Nyquist sampling frequency). Let $\mathbf{h}(t)$ denote a vector that contains all of 2nd-order coefficients $\{h_{kl}(t)\}$; in light of (5), we may compute an *instantaneous* index that quantifies the fractional contribution between the cross-spectrum and the cross-bispectrum [6]:

$$\rho_t \approx \frac{1}{1 + 2|\mathbf{h}(t)| \cdot |\mathcal{D}_{RR}(f, t)|} \quad (6)$$

where $|\cdot|$ denotes either the norm of a vector or the modulus of a complex variable. The “ \approx ” is due to a Gaussian assumption used in deriving (6). A small value of ρ implies a presence of significant (nonzero) values in $\{h_{kl}\}$ (i.e. nonlinearity), whereas a perfect linear Gaussian model would imply $\rho = 1$. (of note, ρ is indicated as **rho** in **figures**)

In light of Eq. (3) we can compute the frequency response for the covariate transfer function (BP→RR or RESP→RR)

$$\tilde{H}_{12}(f, t) = \frac{\sum_{i=1}^q \tilde{b}_i(t) z^{-i} \Big|_{z=e^{j2\pi f_2}}}{1 - \sum_{i=1}^p \tilde{a}_i(t) z^{-1} \Big|_{z=e^{j2\pi f_1}}} \quad (7)$$

where f_1 and f_2 denote the rate (beat/s) for the R-R and covariate intervals, respectively; here we assume $f_1 \approx f_2 \equiv f$ (namely, the heartbeat period is about the same as the covariate-event period). The order of the AR model also determines the number of poles, or oscillations, in the frequency range. Modifying the AR coefficients is equivalent to changing the positions of the poles and reshaping the frequency response curve. With the time-varying AR coefficients $\{\tilde{a}_i(t)\}$ and $\{\tilde{b}_j(t)\}$ estimated from the point-process filter (section D. below), we may evaluate the *dynamic* frequency response of Eq. (7) at different ranges (LF, 0.04–0.15 Hz; HF, 0.15– $\min\{0.5, 0.5/RR\}$ Hz, where $0.5/RR$ denotes the Nyquist sampling frequency). The frequency-dependent transfer function gain, characterized by $|\tilde{H}_{12}(f)|$, represents the effect of the covariate on heartbeat, mediated by the neural autonomic reflex.

In particular, **RSA** and **BRS** (two of the indices shown in figures) are computed from this gain for RESP and BP respectively. Since the R-R interval is influenced by respiratory input at the HF range, it is more common and meaningful to examine the baroreflex gain at the LF range. In light of Eq. (4), we can determine, in the same fashion as (7) and with similar interpretations [8] the differential transfer function

D. Adaptive Point Process Filtering and Goodness-of-Fit

In order to empower the model in a nonstationary environment, we can recursively estimate the parameters via adaptive point process filtering at any time resolution. The state-space formulation of the discrete-time point process filtering algorithm is described in [5,6,7]. The choice of bin size (Δ) reflects the timescale of estimation interest, we often use $\Delta=5$ ms. The point process filtering equations can be viewed as a point process analog of the Kalman filtering equations (for continuous-valued observations). Given a predicted (*a priori*) estimate, the innovations are weighted by an ‘adaptation’ gain to further produce the filtered (*a posteriori*) estimate. Since the innovations are likely to be nonzero in the absence of a beat, the parameters are always updated at each time bin. Goodness-of-fit of all models is evaluated using a Kolmogorov-Smirnov (KS) test based on the time-rescaling theorem, and the transformed quantiles’ autocorrelation function is further computed to check independence of the transformed intervals [5,6,7].

E. Experimental Protocol

A total of 15 healthy volunteer subjects (mean age 24 ± 4) gave written consent to participate in this study approved by the Massachusetts General Hospital (MGH). Intravenous and arterial lines were placed in each subject. Propofol was infused intravenously using a previously validated computer-controlled delivery system running STANPUMP connected to a Harvard 22 syringe pump (Harvard Apparatus, Holliston, MA). Five effect-site target concentrations (0–4 mcg/ml) were each maintained for 15 minutes respectively. Capnography, pulse oximetry, ECG, and arterial BP (P1) were recorded (sampling rate 1 kHz) and monitored continuously by an anesthesiologist throughout the study. Bagmask ventilation with 30% oxygen was administered as needed in the event of propofol-induced apnea. Because propofol is a potent peripheral vasodilator, phenylephrine was administered intravenously to maintain mean arterial BP within 20% of baseline [7].

III. RESULTS

Results on application of our model framework include instantaneous assessment of HRV, RSA, Baroreflex (BRS), and of nonlinear dynamics in healthy subjects under progressive stages of anesthesia [4–8]. All instantaneous indices are estimated to accommodate the nonstationary nature of the experimental recordings. Overall, our observations have revealed interesting dynamic trends across the experiment. We are here showing two original examples:

(1) Figure 1 shows a subject transitioning from level 0 to level 3. Clearly, HRV, RSA and BRS progressively decrease, accompanied by a relevant increase in linear cardiorespiratory coupling as a result of administration of the first propofol bolus (despite the small scale, note the two sharp drops in BRS at the level 1→2 and 2→3 transitions). (2) Figure 2 shows a different subject where, after first propofol administration, phenylephrine is administered to compensate a critical drop in blood pressure, followed by artificial ventilation. Here, a sharp decrease in RSA is observed with anesthetic intervention, respiratory coupling is then partly restored, but blood pressure progressively decreases to critical levels, possibly due to baroreflex failure. After phenylephrine is administered, baroreflex gain and blood pressure slightly recover, but fail to go back to baseline levels. Artificial ventilation reflects in RSA

variability and acts to restore HRV, only partly succeeding in raising blood pressure levels. Table I further shows a statistical summary of levels 1–5 as compared with baseline, accompanied by a portrayal of the instantaneous dynamics observed within each level for the considered indices (Figure 3), confirming the progressive decrease in HRV, RSA and BRS, as well as the linear cardiorespiratory coupling increase in the first two levels of anesthesia.

IV. DISCUSSION

In a non-stationary scenario where the physiological state may change dramatically, dynamic assessment of cardiovascular control during the transient period is of vital importance. Overall, our observations have revealed important dynamics involved with induction of anesthesia. The study of the transient periods due to pharmacological and physical intervention has demonstrated the capacity of the point-process filter to quickly capture fast physiological changes in the cardiovascular system, for example when baroreflex responses are supposedly triggered, and consequently accompanied by a significant drop in the instantaneous baroreflex gain. The clear reduction of BRS with anesthesia might suggest that baroreflex responses are reset with propofol to control HR at a lower BP, and that BRS further decreased after administration as a result. The shift in the HR/BP set point may reflect the propofol's systemic vasodilatory effect, whereas baroreflex impairment is most likely the result of disruption of cardiac control within the central nervous system.

The dynamic estimates further suggest that RSA gradually decreases from baseline after administration of propofol anesthesia, that RSA is generally suppressed by phenylephrine; and that the linear interactions within the cardiorespiratory control remain stable or increase [5]. Specifically, RSA is likely to be mediated by withdrawal of vagal efferent activity resulting from either baroreflex response to spontaneous BP fluctuations, or respiratory gating of central arterial baroreceptor and chemoreceptor afferent inputs. Of note, we also observed an increase of nonlinearity in heartbeat interval dynamics from baseline to anesthesia, where the nonlinearity involved the bilinear interactions between RR and systolic blood pressure (SBP) accompanied by a significant decrease in linear coherence between these two series [7]. This seems to suggest that the nonlinear component of heartbeat interval dynamics during anesthesia is mainly contributed from the cardiovascular (baroreflex) loop, whereas the linear interaction within the cardiorespiratory loop roughly remains unchanged. It is also possible that the respiratory system indirectly influences HR by modulating the baroreceptor and chemoreceptor input to cardiac vagal neurons. However, in our experimental condition, it is difficult to validate the separate influence of SBP from the influence of respiration on HRV.

V. CONCLUSION

A combined point process framework is proposed which enables us to simultaneously assess the linear and nonlinear indices of HRV, together with important cardiovascular functions of interest, in clinical recordings during induction of propofol anesthesia. All of these statistical indices may serve as potential indicators for ambulatory monitoring in clinical practice, and may particularly provide a valuable quantitative assessment of the interaction between heartbeat dynamics and hemodynamics during general anesthesia. More importantly, these quantitative indices could be monitored intraoperatively in order to improve drug administration and reduce side-effects of anesthetic drugs.

Acknowledgments

The authors thank K. Habeeb, G. Harrell, R. Merhar, E. T. Pierce, A. Salazar, C. Tavares and J. Walsh (Massachusetts General Hospital) for assistance with data collection and interpretation.

This work was supported in part by NIH Grants R01-HL084502, K25-NS05758, DP1-OD003646, DP2-OD006454 and R01-DA015644.

REFERENCES

1. Barbieri R, Parati G, Saul JP. Closed- versus open-loop assessment of heart rate baroreflex. *IEEE Mag. Eng. Med. Biol.* 2001; vol. 20(no. 2):33–42.
2. Barbieri R, Matten EC, Alabi AA, Brown EN. A point-process model of human heartbeat intervals: new definitions of heart rate and heart rate variability. *Am J. Physiol. Heart Circ. Physiol.* 2005; vol. 288:424–435.
3. Barbieri R, Brown EN. Analysis of heart beat dynamics by point process adaptive filtering. *IEEE Trans. Biomed. Engin.* 2006; vol. 53(no. 1):4–12.
4. Chen Z, Brown EN, Barbieri R. Assessment of autonomic control and respiratory sinus arrhythmia using point process models of human heart beat dynamics. *IEEE Trans. Biomed. Eng.* 2009; vol. 56:1791–1802. [PubMed: 19272971]
5. Chen, Z.; Purdon, PL.; Pierce, ET.; Harrell, G.; Walsh, J.; Salazar, AF.; Tavares, CL.; Brown, EN.; Barbieri, R. Linear and Nonlinear Quantification of Respiratory Sinus Arrhythmia during Propofol General Anesthesia; *Conf Proc IEEE EMBS*; 2009. p. 5536-5539.978-1-4244-3296-7/09
6. Chen Z, Brown EN, Barbieri R. Characterizing nonlinear heartbeat dynamics within a point process framework. *IEEE Trans. Biomed. Eng.* 2010; vol. 57(no. 6):1335–1347. [PubMed: 20172783]
7. Chen Z, Purdon PL, Harrell G, Pierce ET, Walsh J, Brown EN, Barbieri R. Dynamic Assessment of Baroreflex Control of Heart Rate During Induction of Propofol Anesthesia Using a Point Process Method. *Ann Biomed Eng.* 2011; Vol. 39(1):260–276. [PubMed: 20945159]
8. Chen, Z.; Purdon, PL.; Brown, EN.; Barbieri, R. A Differential Autoregressive Modeling Approach within a Point Process Framework for Non-stationary Heartbeat Intervals Analysis; *Conf Proc IEEE EMBS*; 2010. p. 3567-3570.978-1-4244-4124-2/10

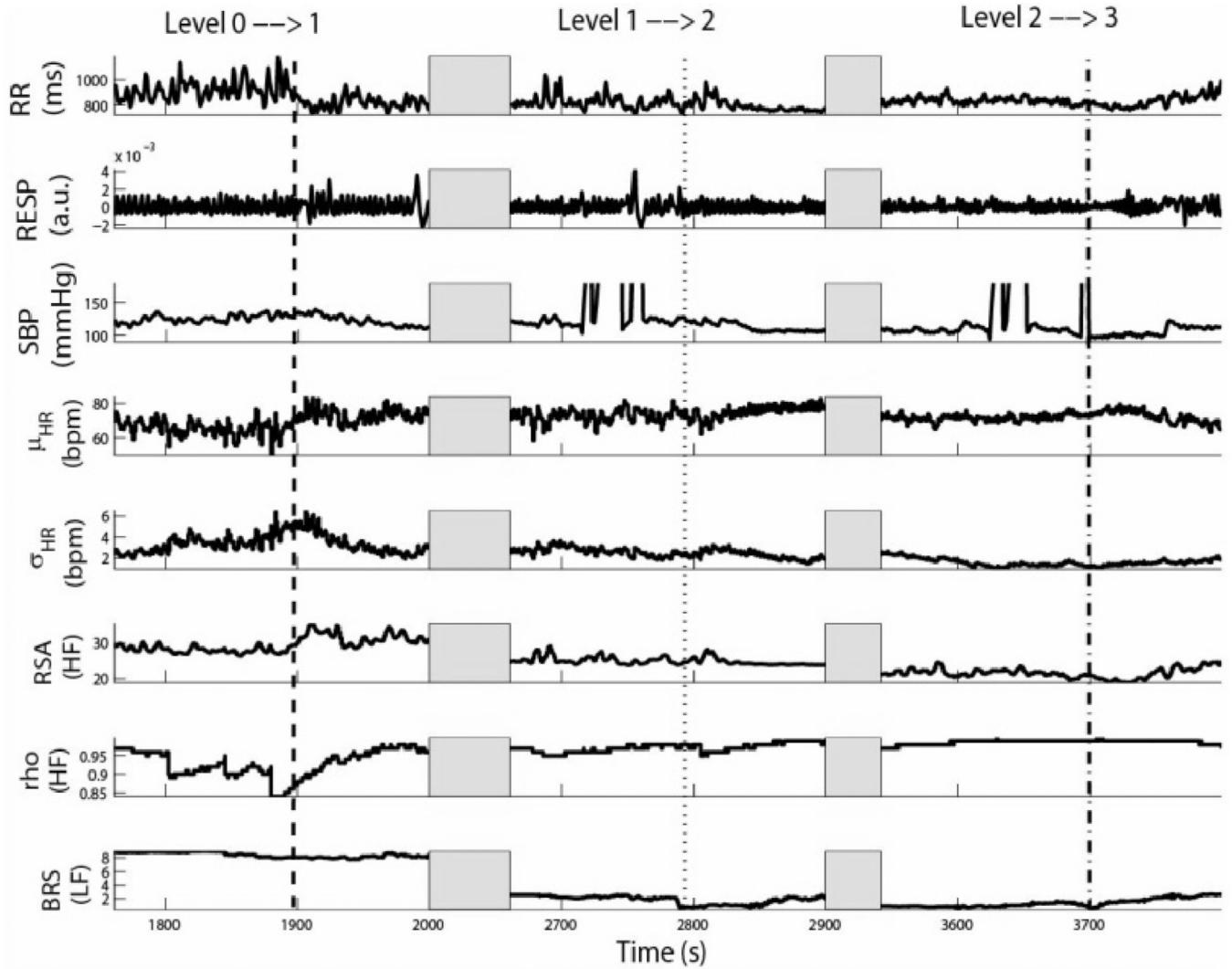


Figure 1.
Tracking results of various instantaneous indices for Subject 15. Three transient periods (level 0→1, level 1→2, level 2→3) are shown.

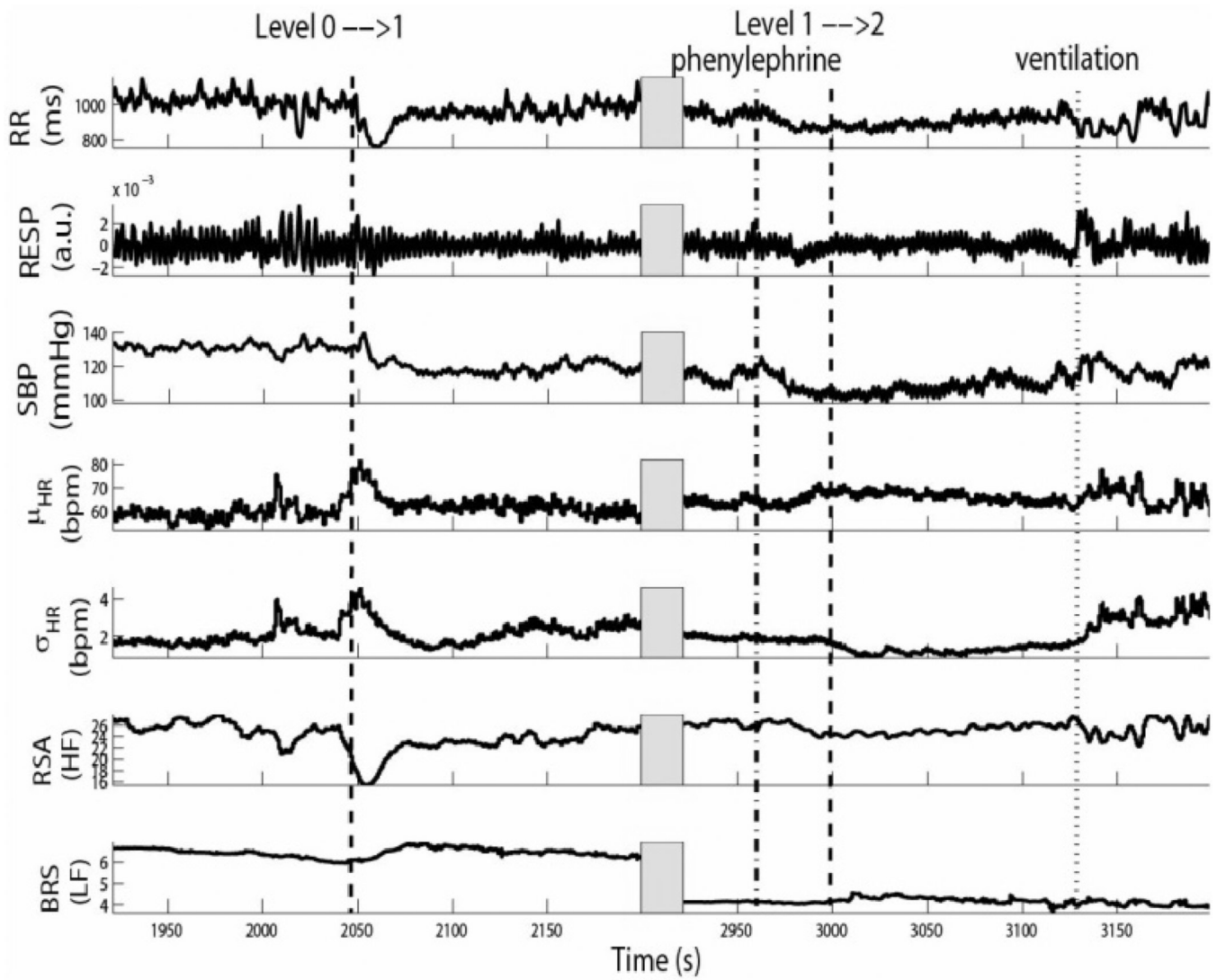


Figure 2.

Tracking results of various instantaneous indices for Subject 9. The two dashed lines (~2050 s and ~3000 s) mark the drug concentration level 0→1, (i.e., propofol administration onset time) and level 1→2, respectively. The dotted dashed line (~2960 s) marks the time when phenylephrine was administered; and the dotted line (~3125 s) marks the time of hand ventilation.

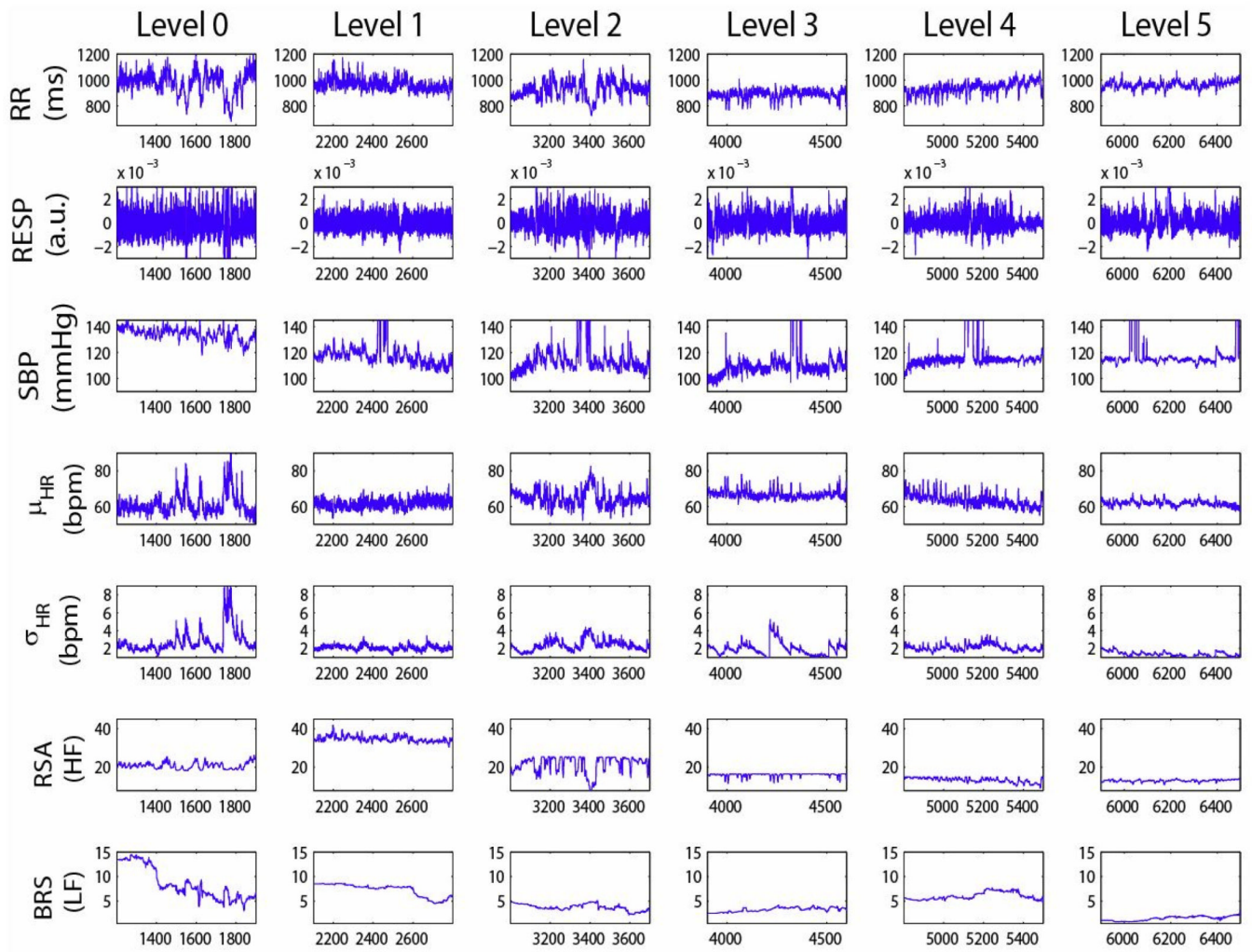


Figure 3.
Estimates of the instantaneous indices for six drug concentration levels (0–5) for Subject 9.

TABLE I

Statistics of the Instantaneous Indices (Subject 9, Levels 0–5)

level	μ_{HR} (bpm)	σ_{HR} (bpm)	RSA (s/a.u.)	Rho (n.u.)	BRS (s/mmHg)
0	61.2±5.8	3.19±.92	20.8±1.7	0.88±.05	8.55±3.24
1	61.8±2.7	2.25±.42*	34.7±1.5*	0.95±.01*	7.33±1.26*
2	64.3±4.1	2.65±1.01	21.6±4.2	0.97±.01*	3.77±.64*
3	67.1±2.5*	1.94±.67	16.1±.85*	0.85±.06	3.28±.42*
4	63.7±3.5	1.98±.29*	13.4±1.3*	0.91±.09	6.05±.75*
5	61.6±2.2	1.71±0.21	13.1±.56*	0.85±.09	1.51±.43*

* significant $P < 0.05$ by pairwise rank-sum test (compared to level 0)